

# Rheological Characteristics of Proanthocyanidin Polymers from *Pinus radiata*. I. Rheological Behavior of Water-Soluble Extract Fractions and Phlobaphenes

SEUNGROK KIM and DAVID E. MAINWARING\*

Centre for Applied Colloid and BioColloid Science, Department of Applied Chemistry, Swinburne University of Technology, Hawthorn 3122, Victoria, Australia

## SYNOPSIS

The rheological characteristics of the solutions of the whole extracts and their fractions from the *Pinus radiata* bark were investigated. The viscosity changes upon addition of aqueous NaOH solution into the solutions of the hot water extracts are due mainly to the dissolution of the phlobaphene fraction. The polyelectrolyte character was established from the solutions of the hot-water extracts. The kinetics of the size growth of naturally forming phlobaphenes could be observed by photon correlation spectroscopy (PCS) from the solutions of hot-water extracts. Mild sonication could degrade phlobaphenes partly and this indicates that the formation of phlobaphenes is partly associated with colloidal interaction. © 1995 John Wiley & Sons, Inc.

## INTRODUCTION

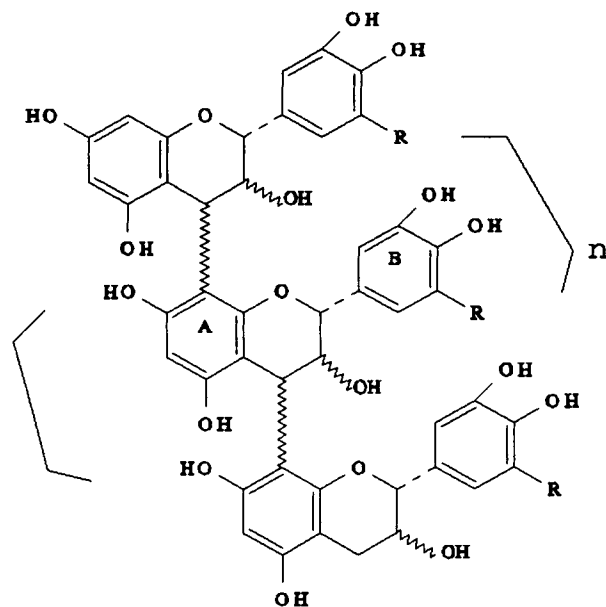
Proanthocyanidin polymers (condensed tannins) occur in the bark of all conifers and hardwoods examined to date, and they are frequently present in wood.<sup>1</sup> Proanthocyanidin polymers consist of linear chains of flavan-3-ol units that have undergone varying degrees of condensation,<sup>2,3</sup> as illustrated in Figure 1.

While the majority of proanthocyanidins consist of both procyanidins and prodelphinidins, Czochanska et al.<sup>3</sup> showed that *Pinus radiata* (*P.r.*) bark consists of a ratio of 90 : 10 of these respective analogs. The number-average molecular weight ( $M_n$ ) for *P.r.* proanthocyanidins was found to be 1740.<sup>3</sup> The phenolic components of the proanthocyanidin polymers are important to adhesive chemistry because they have reactive sites available for condensation with formaldehyde.<sup>4</sup> The primary characteristic of the water-soluble proanthocyanidin polymers is dehydration/oxidation to intensely colored anthocyanidin pigment<sup>1</sup> when refluxed in butanol and hydrochloric acid. For this reason, there has been a

tendency to refer to these polyhydric phenol (polyphenol) compounds as "proanthocyanidins."<sup>1</sup> Another characteristic of the proanthocyanidin polymers is the formation of "phlobaphenes" after extraction. These substances, although initially soluble in water, become insoluble in water as they associate with each other. They can, however, be dissolved in polar solvents such as ethanol and acetone or in an aqueous base. Phlobaphenes can be easily precipitated from the water solution of proanthocyanidin polymers by acid-induced condensation reactions. Some phlobaphenes are formed spontaneously and are complex mixtures of high molecular weight proanthocyanidin polymers which have, in some instances, been found to be associated with carbohydrates.<sup>5</sup>

Generally, the polyphenols derived from the hot-water extract of a bark or heartwood were considered to consist of about 60–65% proanthocyanidin polymers as measured by a standard hide powder absorption test.<sup>1</sup> The remainder was considered to be a mixture of sugars, pectin, hemicellulose, and low molecular weight ( $\leq 300$ ) polyphenols. Carbohydrate impurities are considered extraneous substances; thus, there has been considerable research effort aimed at identifying particular plant species that yield an extract of high polyphenol content and low

\* To whom correspondence should be addressed.



- (a) R=H, procyanidin units (PC)  
 (b) R=OH, prodelphinidin units (PD)

Figure 1 Structure of proanthocyanidins.

in the carbohydrate "contaminants." In spite of the maturity of the study of plant-derived polyphenols and the increasing number of unequivocal molecular structures being established, the complexity of the interactions involved in their condensation and aggregation has made it difficult to overcome limitations to their technological application.

A recent study of Sealy-Fisher and Pizzi<sup>6</sup> showed that phlobaphene formation and precipitation during sulfite/water extraction of polyphenols from *P.r.* bark was minimized by preventing polyphenol self-condensation via the addition of a strong nucleophile such as phloroglucinol, *m*-phenylenediamine, and urea. These inhibitors were found to react preferentially with the reaction intermediates formed by the self-condensation mechanism of the polyphenols, thereby inhibiting the molecular rearrangement leading to phlobaphene precipitates.

It was previously shown that the aqueous extract of the *P.r.* bark contains polyhydric phenols (Fig. 1) that are polyflavonoid in nature<sup>7</sup> and that these extracts form the basis of wood adhesives.<sup>8</sup> However, industrial processes have been hindered largely because of a number of problems associated with high chemical reactivity, relative instability in solution, and excessive viscosity of high-yield extracts, although a small producer of natural and sulfited *P.r.* extracts has commenced industrial production.<sup>9</sup>

Pizzi et al. studied the underlying chemistry of the formulation used in these processes.<sup>9</sup> It is important to understand the contribution of each fraction of the extracts to the flow behavior if the limitations of viscosity are to be addressed. The stability and rheological characteristics of the extracts vary significantly depending on the extraction method, since different fractions may be isolated by different extraction methods. Many of the limitations in the use of bark extracts remain centered on an inadequate understanding of the factors that influence the resulting complex rheological characteristics.

## APPROACH

The hot-water extracts (100°C; HWE) from the *P.r.* bark were investigated over a range of concentrations which included various contents of the solubilized phlobaphenes (dissolved by aqueous NaOH solution) by dilute solution viscometry and photon correlation spectroscopy (PCS). These components of the HWE were compared with a pure phlobaphene fraction solubilized by aqueous NaOH solution which had precipitated at room temperature from the HWE and was isolated by centrifugation. The cold-water extracts (20°C; CWE) were also compared with HWE solutions without solubilized phlobaphenes by dilute solution viscometry and steady-shear rotational viscometry to identify their contribution to the flow characteristics. Since the HWE showed significant polyelectrolytic behavior in the presence of the solubilized phlobaphenes at high pH, ionic effects of the alkali salts of the HWE were investigated by measuring viscosities at various background electrolyte concentrations.

## EXPERIMENTAL

### Sample Preparation

Yazaki<sup>10</sup> reported previously that the yield of extract from the *P.r.* bark depends on the particle size at which the extraction was carried out. Table I shows cumulative size distribution of dried bark powder used for all extractions. The sample preparation procedures of either the extracts or their fractions are depicted in the scheme shown in Figure 2.

### 20°C Extraction

Distilled water (500 mL) at 20°C was added to 100 g of dried *P.r.* bark powders in a beaker. The suspension was stirred vigorously for 10 min to extract

**Table I** Size Distributions of Bark Powder Used for Extraction

Screen Size ( $\mu\text{m}$ )	Cumulative % Oversize
850	100.00
425	98.02
212	68.22
106	27.27
53	10.39
-53	6.00

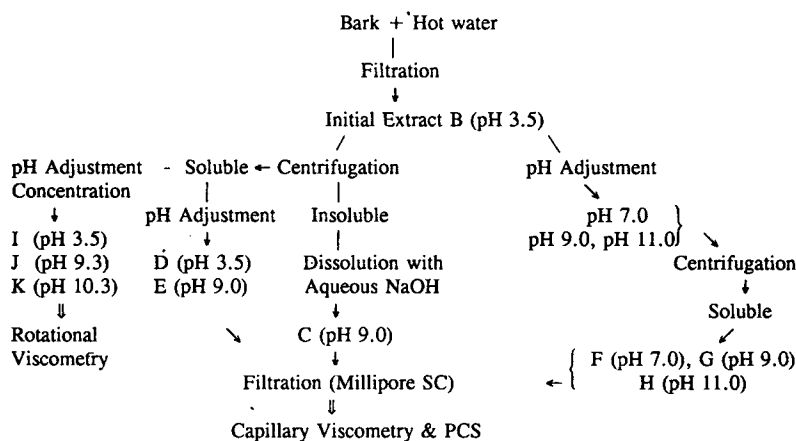
the polyphenols and then filtered using a Buchner funnel and No. 41 Whatman filter paper to remove the insoluble materials. Yields were recorded and calculated on a dry-bark basis as determined by air-oven drying at 105°C. Filtrates were centrifuged at 4000 rpm for 30 min to isolate possible insolubles, but no precipitates were observed. The extract was then filtered through an 8.0  $\mu\text{m}$  Millipore SC filter for dilute solution viscometry. Since storage of the

transparent extracts gave a precipitate by molecular association, all experiments were carried out on the fresh solution of the extract (sample A, pH 3.6) prior to the formation of precipitates. Part of the CWE was concentrated after centrifugation for rotational viscometry (samples L, M, and N). The dilute extract solutions were concentrated by evaporation at 40°C to minimize autocondensation.

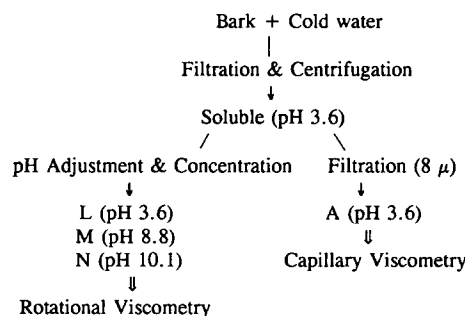
### 100°C Extraction

Distilled water (500 mL) at 100°C was added to 100 g of dried *P.r.* bark powder and stirred vigorously for 10 min prior to filtering similarly with a Buchner funnel and No. 41 Whatman filter paper to remove insoluble materials. After filtration, identical aliquots from the extract (sample B; pH 3.5) were introduced into various sample bottles and the pH adjusted to 7, 9, and 11, respectively, with a 0.5N NaOH solution. The insoluble parts of the extracts were isolated by centrifugation for 30 min at 4000 rpm after pH adjustment and the soluble fractions

(a) Hot Water (100°C) Extraction



(b) Cold (20°C) Water Extraction

**Figure 2** Experimental scheme for 100°C water extraction and 20°C water extraction.

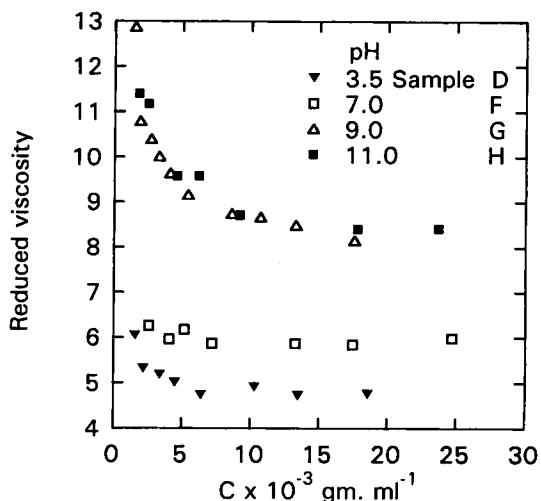


**Figure 3** Reduced viscosity of the HWE vs. extract concentration with different amounts of dissolved phlo-baphene fraction.

obtained. The insoluble fraction isolated from Sample B was solubilized with a 0.5N NaOH solution and the pH was adjusted to 9 (sample C). Storage of these transparent supernatants produced second precipitates by both autocondensation<sup>11</sup> and colloidal or molecular association.<sup>12</sup> Thus, all experiments were again carried out on the fresh samples before the formation of precipitates.

## Characterization

### Capillary Viscometry

Viscometric measurements were carried out after filtration with a 8.0  $\mu\text{m}$  Millipore filter with an Ubbelohde dilution viscometer similar to Pizzi and Vogel<sup>13</sup> who related intrinsic viscosity to the degree of polymerization of tannin-formaldehyde. The viscometer and sample were maintained at a temperature of  $20 \pm 0.1^\circ\text{C}$ . A capillary of 0.64 mm diameter was used. Samples were also examined with capillaries of different sizes to evaluate any shear-rate effects. The efflux time was measured for a set volume to flow through the capillary and repeated at least five times. The flow time for conductivity water was 159.4 s and the kinetic energy correction was therefore neglected.

### Quasi-Elastic Light-Scattering (QELS) Measurements

All QELS measurements were carried out in a photon correlation spectroscopy (PCS) mode using a Model N4 MD submicron particle analyzer (Coulter

Electronics). The photomultiplier assembly was positioned at  $62.3^\circ$  to the incident laser beam. A helium-neon laser operating at 632.8 nm was used as the scattering source. An incident intensity of 4 mW was employed. Diffusion coefficients were extracted from the autocorrelation functions by use of the regularization program CONTIN.<sup>14</sup> Hydrodynamic radii were then calculated by applying the Stokes-Einstein relationship

$$r = k_B T / 6\pi\eta_0 D_z$$

where  $r$  is the Stokes radius;  $k_B$ , the Boltzmann constant;  $\eta_0$ , the viscosity of the solvent; and  $D_z$ , the  $z$ -averaged translational diffusion coefficient,<sup>15</sup> determined at the measurement temperature ( $T$ ) of  $20^\circ\text{C}$ .

The model N4 MD system employs a size-distribution processor (SDP) system that utilizes CONTIN to calculate particle-size distributions. The SDP and CONTIN analysis methods were utilized for the characterization of association of the extract solutions as a function of time. Standard Teflon-stoppered spectrophotometric cuvettes were employed as scattering cells and the cell was ultrasonically cleaned and flushed several times with double-distilled water filtered with a 0.22  $\mu\text{m}$  Millipore syringe filter (Sterile Millex-GV) to remove any dust particles. The cell was further rinsed with a filtered (0.22  $\mu\text{m}$  Millipore syringe filter) diluent and filled with a 3 mL filtered diluent. Approximately 0.025 mL of the appropriate extract solution (2% w/v) was introduced into the cell via an 8  $\mu\text{m}$  Millipore syringe filter (Millipore-SC) to achieve the

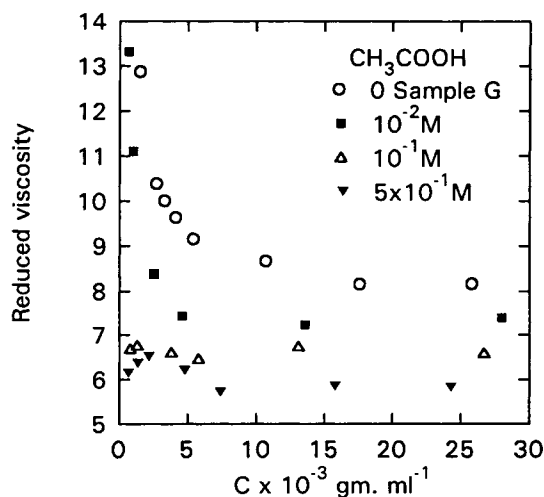


**Figure 4** Reduced viscosity of the solution of the HWE vs. extract concentration at different acetic acid concentrations.

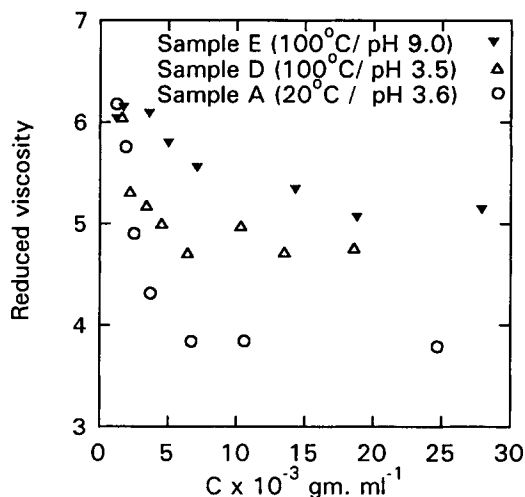


**Figure 5** Reduced viscosity of HWE at pH values of 3.5 and 9 (no dissolved phlobaphene) and reduced viscosity of CWE (pH 3.6) without dissolution of phlobaphene fraction vs. extract concentration.

desired intensity of scattered light. Since these relatively dilute solutions of extracts scatter light weakly, it was necessary to employ a scattering angle below  $90^\circ$ . Each experiment was repeated several times to assure reproducibility.

### Rheological Measurements

Rheological parameters were measured at  $20 \pm 0.1^\circ\text{C}$  with a Rheometrics Fluid Spectrometer RFS II (Rheometrics, Piscataway, NJ) equipped with a concentric Couette geometry (cup radius: 17 mm; bob radius: 16 mm; bob length: 34 mm). Throughout the experiments, the torque sensitivity was varied by a decade by changing the mode of the force-rebalanced transducer.

## RESULTS AND DISCUSSION

The yield of natural HWE produced without additives was 11.65% (w/w) on the basis of the weight of original dried *P.r.* bark and the pH of the original extract was 3.5. As stated previously, the soluble fraction (sample D) of the HWE (sample B) gradually formed insoluble phlobaphene precipitates over a period of days at room temperature. The phlobaphenes formed at low pH, although soluble initially, could not be totally redissolved, unless the pH was increased beyond 9. Thus, it can be seen from Figure 2(a) that samples D and F represent the soluble fractions at pH values of 3.5 and 7.0, respectively, while samples G and H represent the whole initial

extract (sample B) at pH values of 9.0 and 11.0, respectively. Hence, the progression in the sample series D–F–G–H represents increasing amounts of dissolved phlobaphenes.

Generally, pH regulates the charge of polyelectrolyte macromolecules and, thus, the magnitude of the Coulombic interactions, which are subsequently screened by the counterions of the background electrolyte solution. The situation, however, is different in the present study, since pH was adjusted initially in the presence of phlobaphene, leading to a greater dissolution of the phlobaphene fraction as pH increases. Thus, the increase in the reduced viscosities in Figure 3 appears to be primarily a function of the dissolution of hot-water insoluble fractions, i.e., higher molecular weight materials which were solubilized from the phlobaphenes by alkaline solution are responsible for the higher reduced viscosity. The significant increase in both the high concentration plateau viscosity and the concave rise in viscosity upon dilution at pH values of 9 and 11 suggests that the phlobaphene fraction is not merely a simple high molecular weight analog of water-soluble polyphenols but, rather, a complex mixture with water-insoluble polymers which are unrelated to the proanthocyanidin family, since alkali has been shown to convert water-insoluble polyphenols to lower molecular weight fractions by acting as a nucleophile,<sup>16</sup> although Pizzi and Stephanou<sup>11,17</sup> found that rapid autocondensation and recombination occurs.

The reduced viscosity curves in Figure 3 are strongly concave upward at lower concentrations, in marked contrast to the behavior of uncharged linear polymers. It is notable that the sharp rise in

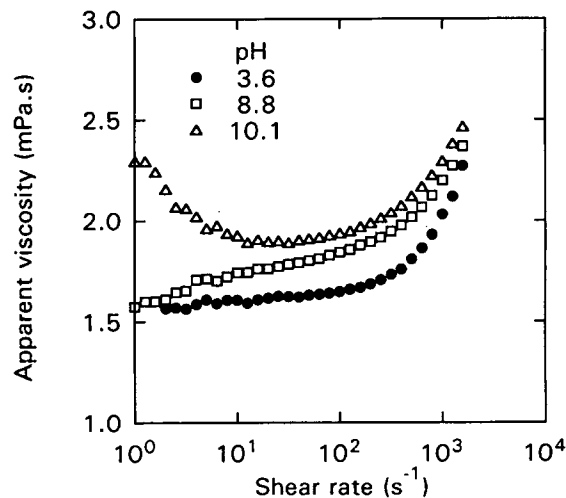


**Figure 6** Viscosity flow curves of 11.7% CWE at three different pH's (samples L, M, and N).

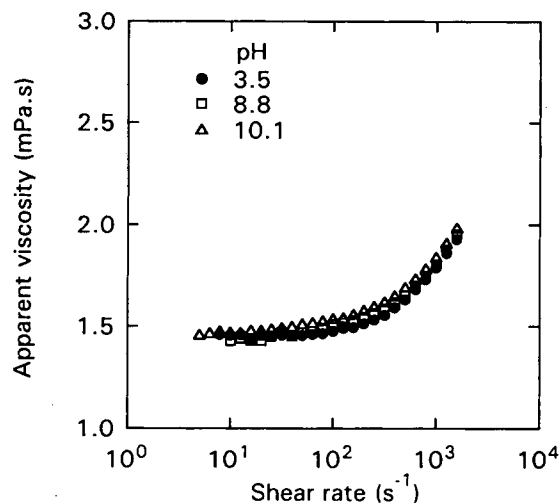


**Figure 7** Viscosity flow curves of 7.6% HWE at three different pH's (samples I, J, and K).

viscosity of the extract solutions as the concentration tends to zero occurs with increasing dissolution of NaOH-soluble phlobaphene fraction. Similar behavior is shown at pH 9 and 11, since full dissolution of phlobaphene had occurred by pH 9. The increase in the reduced viscosity ( $\eta_{sp}/c$ ) with dilution of a polymer was attributed by Fuoss and Strauss<sup>18</sup> to the reduction in the degree of ionic association between the polyion and its counterions. With dilution, the degree of counterion association becomes reduced by a mass-action effect and the effective net charge on the polymer increases. The molecular extension due to intrachain electrostatic repulsion causes the reduced viscosity to increase.<sup>19</sup> This polyelectrolytic behavior of the extract solutions of *P.r.* bark and other similar extraction products has not been reported previously. Figure 3 also shows a significant shift in the end of the plateau region as the onset of chain expansion shifts to higher concentrations at the higher pH values, indicating greater intramolecular repulsion due to higher charge densities on the chain.

Ionic interactions in these solutions of the HWE were further investigated by measuring viscosities at various background electrolyte concentrations. Figure 4 shows the dependence of the reduced viscosity on the extract concentration at different acetic acid concentrations. When the extract is dissolved in aqueous NaOH solution at pH 9 (sample G), the reduced viscosity increases with a decrease in extract concentration, as discussed. As the concentration of acetic acid increases from  $10^{-2}$  to  $10^{-1}M$ , the sharp rise in reduced viscosity is progressively eliminated, and the curve exhibits a slight maximum. Intra-

molecular repulsion is thus reduced by both protonation of the charged groups and compression of the electrical double layer due to the increased proton population in the electrolyte at low pH values. A further increase of the concentration of acetic acid to  $5 \times 10^{-1}M$  induced a more significant maximum in the curve. Fuoss and Strauss<sup>18</sup> suggested that the maximum appears when the stoichiometric concentration of ions from the polymer is of the same order of magnitude as that of the co-ion concentration of the medium.

To further establish that these reduced viscosity results in Figure 3 are indeed representative of molecular size, we compared in Figure 5 three samples not containing phlobaphenes, i.e., the soluble portion of the HWE at the initial pH 3.5 (sample D), the soluble part of the CWE (sample A) at the initial pH 3.6, and HWE at pH 9 (sample E). Comparison of the solutions of the components that contain no phlobaphenes, i.e., HWE at pH 3.5 and 9, indicates that the electrostatic contributions to viscosity, due to an increased charge density on the chain and as shown by the change in the plateau reduced viscosity ( $\Delta\eta_{red}$ ), is relatively small ( $\Delta\eta_{red} = 0.4$ ). This result confirms that the water-insoluble polymers which are not simple polymers of the monomers and oligomers of the water-soluble extracts are mainly responsible for the significant increase in viscosity at high pH shown in Figure 3 where  $\Delta\eta_{red} = 3.5$ . This is also supported by the reduced viscosity converging (at 6.2) as polymer concentration approaches zero, unlike the behavior in Figure 3. Figure 5 also suggests that higher purity polyphenol extract<sup>1</sup> (CWE)

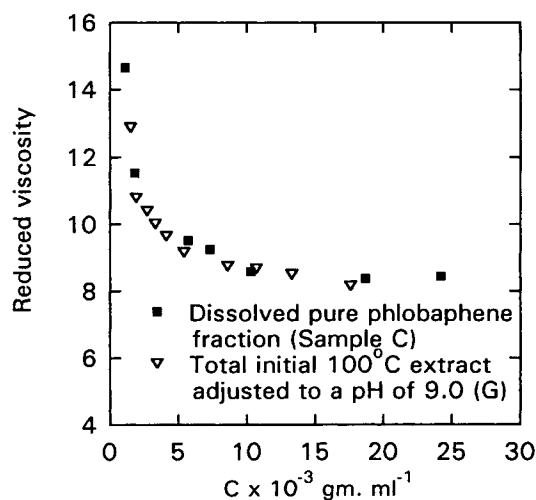


**Figure 8** Reduced viscosity of dissolved pure phlobaphene fraction (sample C) and initial HWE adjusted to a pH of 9 (sample G), respectively.

**Table II** A Comparison of an Average Diffusion Coefficient for Various Fractions of HWE at pH 9

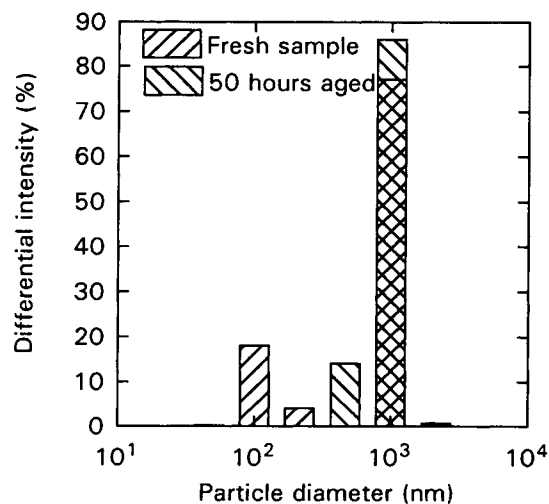
Extracts (pH 9)	Translational Diffusion Coefficient ( $\times 10^{-9}$ cm <sup>2</sup> /s)
Sample G (pH adjusted in the presence of phlobaphene)	8.93
Sample E (phlobaphene removed before pH adjustment)	8.98
Sample C (phlobaphene portion isolated and dissolved)	4.36

results in a lower viscosity due to the absence of extraneous substances. Notably, the overall yield of CWE also became lower (5.95% w/w). Phlobaphene formation was considerably reduced in the CWE as it took at least 2 days to observe the presence of phlobaphene precipitates. The formation of phlobaphene from HWE was instantaneous after extraction. Figure 5 indicates that higher molecular weight distributions of the aqueous extracts could be obtained at higher temperature during the extraction process. Yazaki and Hillis<sup>20</sup> determined the molecular size distribution of the aqueous extracts from *P.r.* prepared at different temperatures and their size estimates are consistent with the viscosity results shown in Figure 5.

The relatively small increase in viscosity of the HWE (samples D and E) with a change in pH from 3.5 to 9 shown in Figure 5 was further investigated by Couette rotational viscometry in Figures 6 and 7. Figure 6 indicates the electrostatic contribution to the apparent viscosity of the 11.7% (w/w) solutions of CWE. At the natural extraction pH (3.6), the solution demonstrated at shear rates below 100 s<sup>-1</sup> Newtonian behavior, i.e., shear-independent viscosity. Apparent viscosity increases only slightly as pH increases. However, it is meaningful to note the study of Hemingway et al.<sup>21</sup> in which procyanidin polymers are shown to be rapidly converted at ambient temperatures to species where most of the flavan-3-ol units contain a rearranged A-ring (to the catechinic acid arrangement) in strongly alkaline solutions. On this basis, it was proposed<sup>22</sup> that procyanidins are converted to chains with a greater degree of rigidity than that of the original polymer; however, recent <sup>13</sup>C-NMR work on the tannins themselves indicate that they do not account for more than 1–2% of the total mass of the tannin ex-

tract.<sup>11</sup> In this respect, the slight increase of apparent viscosity with increasing pH in Figure 6 is probably due to limited autocondensation or colloidal association. Notably, all extract solutions showed a significant onset of shear thickening at approximately 100 s<sup>-1</sup>. At shear rates below about 100 s<sup>-1</sup>, slight shear thinning occurred for the structured "at rest" solution at the highest pH (10.1), whereas at the lower pH of 8.8, this structuring "at rest" does not occur and the apparent viscosity is lower. As the shear rate is increased, this solution shows the immediate onset of slight shear thickening, which is absent at the lowest pH (3.6). Distortion of the electrical double layer in the shear field provides an increasing resistance to flow and, hence, an increasing apparent viscosity which scales with both charge density on the chain (pH) and shear field (shear rate), leading to the shear thickening associated with the primary electroviscous effect. Thus, the structured solution (at highest pH) has a high zero shear viscosity together with a high degree of shear sensitivity (non-Newtonian shear thinning) that, once broken, gives a resulting solution that is susceptible to the shear-thickening processes of the primary electroviscous effect similar to the other solutions.

Figure 7 indicates that the electrostatic contribution has little influence on the apparent viscosity of the HWE solutions. For all pH conditions, the HWE showed Newtonian behavior at the lowest shear rate, with the onset of pronounced shear thickening similarly occurring at about 100 s<sup>-1</sup>. The more complex behavior with pH of the CWE compared to the HWE is consistent with Figure 5, where it can be seen that the CWE undergoes substantially

**Figure 9** Size distribution of HWE at pH 3.5 as a function of time.

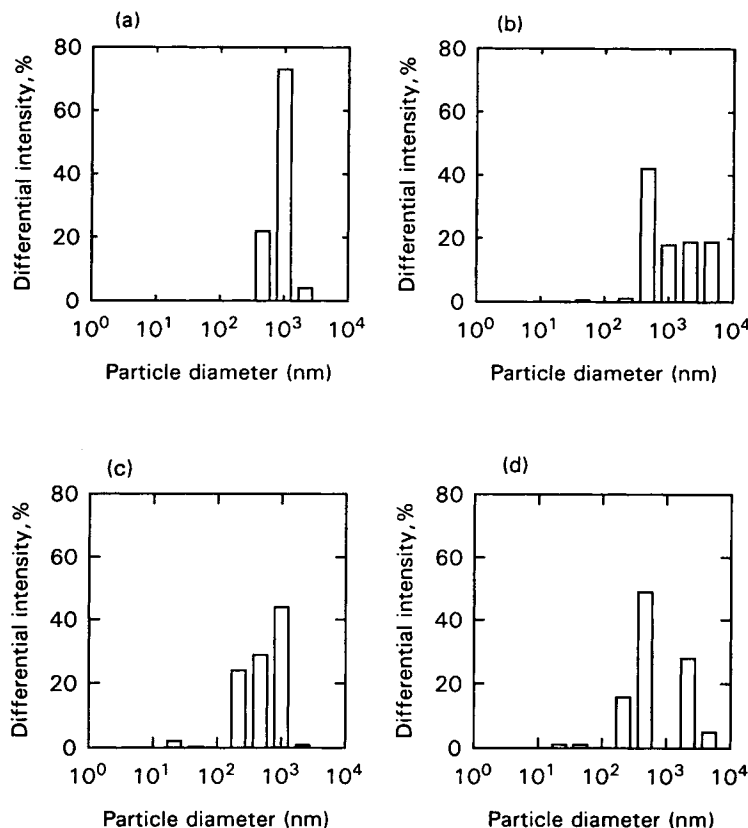


**Figure 10** The kinetics of aggregate formation of HWE at pH 8 and the impact of ultrasound as observed by PCS: (a) fresh sample; (b) 75 h aged; (c) sonicated after 76 h; (d) 9 h aged after sonication.

higher chain expansion upon dilution compared to the HWE at a similar pH. This is indicative of the higher charge density of the CWE macromolecule and consistent with its ability to be solubilized in water even at 20°C.

The dominant contribution of NaOH soluble phlobaphenes to the solution viscosities seen in Figure 3 is again confirmed in Figure 8 by comparing the insoluble portion of the initial extract dissolved at a pH of 9 (sample C) with total initial HWE adjusted to a pH of 9 (sample G). Figure 8 demonstrates pronounced polyelectrolytic behavior of the pure phlobaphene fraction. The significant increase in the reduced viscosity brought about in Figure 3 by dissolution at high pH values was attributed to an increasing proportion of phlobaphenes in solution. This was confirmed in Figure 8 by the identical reduced viscosity of the pure phlobaphene samples, indicating little influence from accompanying water-soluble extracts.

The diffusion coefficient of each fraction responsible for the variation of reduced viscosity was measured at 20°C. The resulting values of the average

diffusion coefficient for the different fractions of the HWE are given in Table II. These results indicate directly that the phlobaphene fractions in the extract solutions consist of long-chain polymers. These long-chain polymers of phlobaphene with their ionizable groups distributed along the chain are a necessary condition for the sharp rise with decreasing concentration as seen in Figure 3.

As noted, storage of the transparent supernatant (centrifuged and filtered HWE) produced a second precipitate. With storage, the size of the soluble polymer increased progressively. PCS was used to study the kinetics of this growth in size. As shown in Figure 9, the soluble fraction at pH 3.5 (sample D) increased in hydrodynamic diameter over time until species with diameters of microns dominated the light scattering in the solution. A similar effect was observed in the extract at pH 8, where a significant change in the size distribution was observed after 75 h [Fig. 10 (a) and (b)]. It is also clearly observed in Figure 10(c) that ultrasound can partly degrade aggregates that form through noncovalent linkages. The aggregation process was observed to

reoccur after sonication, as shown in Figure 10(d). The results in Figures 9 and 10 indicate that the individual molecular species, molecular clusters, or particles may be joined by partial self-condensation,<sup>17</sup> van der Waals attractive association, and/or molecular entanglement. The addition of compounds such as urea,<sup>6</sup> which can act as hydrogen-bond breakers, reduce the viscosity of the extracts, and this indicates that hydrogen bonding is a factor<sup>23</sup> in the aggregation of the *P.r.* extracts.

## CONCLUSIONS

The viscosity changes produced by the addition of aqueous NaOH solution into the solutions of the 100°C water extracts of *Pinus radiata* bark are due mainly to the solubilization of the phlobaphene fraction. The solutions of the hot-water extracts exhibited pronounced polyelectrolyte characteristics with the reduced viscosity curves were strongly concave-upward near zero concentration with increasing dissolution of phlobaphenes. PCS could be used to study the kinetics of the size growth during storage. The size of the soluble fraction increased over time until particles in the micron-size range dominated the light scattering of the solution. Ultrasound could degrade these aggregates partly, indicating the presence of noncovalent linkages and the aggregation process was observed reoccur after sonication.

We thank Chem. Eng. Contracts Pty. Ltd. for their generous supply of the *Pinus radiata* bark powders used in this study. The authors would like to thank the Australian Research Council for the award of an ARC industrial collaborative research grant in support of this work.

## REFERENCES

1. H. L. Hergert, in *Adhesives from Renewable Resources*, R. W. Hemingway, A. H. Conner, and S. J. Branham, Eds., ACS Symposium Series 385, American Chemical Society, Washington, DC, 1989, Chap. 12.
2. D. E. Hathaway, in *Wood Extractives and Their Significance to the Pulp and Paper Industries*, W. E. Hillis, Ed., Academic Press, New York, 1962, Chap. 5.
3. Z. Czochanska, L. Y. Foo, R. H. Newman, and L. J. Porter, *J. Chem. Soc. Perkin Trans. 1*, 2278–2286 (1980).
4. W. E. Hillis and G. Urbach, *J. Appl. Chem.*, **9**, 665–672 (1959).
5. L. Y. Foo and J. J. Karchesy, *Chemical Nature of Phlobaphenes*, R. W. Hemingway and J. J. Karchesy, Eds., Plenum Press, New York, 1989.
6. V. J. Sealy-Fisher and A. Pizzi, *Holz Roh Werkstoff*, **50**, 212–220 (1992).
7. R. W. Hemingway, in *Proceedings of Complete Tree Utilization to Southern Pine Symposium*, New Orleans, April 17–19, 1978.
8. E. P. von Leyser and A. Pizzi, *Holz Roh Werkstoff*, **48**, 25–29 (1990).
9. A. Pizzi, E. P. von Leyser, J. Valenzuela, and J. G. Clark, *Holzforschung*, **47**(2), 168–174 (1993).
10. Y. Yazaki, *Holzforschung*, **39**(5), 267–271 (1985).
11. A. Pizzi and A. Stephanou, *J. Appl. Polym. Sci.*, **51**, 2109–2124 (1994).
12. A. Pizzi and A. Stephanou, *J. Appl. Polym. Sci.*, **51**, 2125–2130 (1994).
13. A. Pizzi and M. C. Vogel, *J. Macromol. Sci.-Chem. A*, **19**(3), 389–397 (1983).
14. S. W. Provencher, *Comput. Phys. Commun.*, **27**, 213–227, 229–242 (1982).
15. J. C. Thomas, *J. Colloid Interface Sci.*, **117**(1), 187–192 (1987).
16. P. E. Laks and R. W. Hemingway, *J. Chem. Soc. Perkin Trans. 1*, 465–470 (1987).
17. A. Pizzi and A. Stephanou, *Holzforsch. Holzverwert.* **45**(2), 30–33 (1993).
18. R. M. Fuoss and U. P. Strauss, *J. Polym. Sci.*, **3**(4), 602–603 (1948).
19. B. E. Conway and A. Dobry-Duclaux, in *Rheology—Theory and Applications*, F. R. Eirich, Ed., Academic Press, New York, 1960, Chap. 3, p. 108.
20. Y. Yazaki and W. E. Hillis, *Holzforschung*, **34**, 125–130 (1980).
21. P. E. Laks, R. W. Hemingway, and A. H. Conner, *J. Chem. Soc. Perkin Trans. 1*, 1875 (1987).
22. L. J. Porter, in *Adhesives in Renewable Resources*, R. W. Hemingway, A. H. Conner, and S. J. Branham, Eds., ACS Symposium Series 385, American Chemical Society, Washington, DC, 1989, Chap. 13, pp. 172–184.
23. Y. Yazaki, *Holzforschung*, **38**, 79–84 (1984).

Received May 26, 1994

Accepted October 21, 1994